

1 Article: <https://www.sciencedirect.com/science/article/pii/S1352231020307184>

2 pre-production copy

3 Synoptic weather and surface ozone concentration in South Korea

4 Hyun Cheol Kim^{1,2,†}, Dasom Lee^{3,†}, Fong Ngan^{1,2}, Byeong-Uk Kim⁴, Soontae Kim⁵, Changhan Bae⁶, and Jin-Ho Yoon³

5 ¹ Air Resources Laboratory, National Oceanic and Atmospheric Administration, College Park, MD, USA

6 ² Cooperative Institute for Satellite Earth System Studies, University of Maryland, College Park, MD, USA

7 ³ School of Earth Sciences and Environmental Engineering, Gwangju Institute of Science and Technology, Gwangju,
8 South Korea

9 ⁴ Georgia Environmental Protection Division, Atlanta, GA, USA

10 ⁵ Department of Environmental and Safety Engineering, Ajou University, Suwon, South Korea

11 ⁶ National Air Emission Inventory and Research Center, Cheongju, South Korea

12 † Both authors contributed equally

13 Correspondence to: Hyun Cheol Kim (hyun.kim@noaa.gov), Jin-Ho Yoon (yjinho@gist.ac.kr)

14 **Abstract.** Seventeen years (2001–2017) of surface observations and spatial synoptic classification (SSC) data are
15 used to analyze the characteristics of surface ozone concentration according to synoptic weather patterns. While
16 weather conditions are known to play an important role in regional air quality, the extent to which synoptic
17 weather patterns affect the production of high ground-level ozone concentrations has not yet been fully
18 quantified. Using thermal characteristics and geographic origins, the SSC method classifies air masses into six
19 types: dry polar (DP), dry moderate (DM), dry tropical (DT), moist polar (MP), moist moderate (MM), and moist
20 tropical (MT). We link daily maximum eight-hour ozone concentrations (MDA8 O₃) from 306 monitoring sites to
21 the closest SSC classifications at 17 airport sites and then analyze their association. We find that DM, DT, and MT
22 are commonly associated with high ozone, whereas DT produces ozone with the greatest efficiency, especially high
23 levels of concentration. This finding implies a potentially strong connection between surface ozone and climate
24 change because the occurrence of DT weather has increased by more than three times over the past 50 years in
25 South Korea. Sensitivity tests reveal that mean MDA8 ozone may increase by 3.5% (7.5%) as the DT frequency
26 increases by 200% (300%). The impacts are larger for higher levels of concentration, with 31.7% (63.3%) or more
27 prevalence of the >80 ppb range with the same increased DT frequency. We conclude that synoptic weather and
28 its long-term trends play important roles in the increased surface ozone recently seen in South Korea.

29 1. Introduction

30 Surface ozone (O₃), one of the important trace gases in the troposphere, is formed from photochemical reactions
31 between two major air pollutants, oxides of nitrogen (NO_x) and volatile organic compounds (VOCs). Heat and solar
32 radiation are also critical in the formation of ozone, resulting in clear seasonal variation: higher ambient ozone
33 concentrations during warmer months and lower concentrations in colder months. Local ozone production is
34 affected by many factors, including anthropogenic sources, such as NO_x and VOCs emissions from mobile,
35 industrial (Bae et al., 2018), and power generation facilities, and natural sources, such as biogenic VOCs emissions
36 (E. Kim et al., 2017). Meteorological conditions are also critical, because ozone photochemistry is basically photon-
37 limited, sensitive to supplied ultraviolet actinic fluxes (Kim et al., 2015). Warm and dry air (i.e., less cloud and more
38 sunlight) favors the production of surface ozone (Bloomer et al., 2009; Camalier et al., 2007; Ryan et al., 1998).

39 Like other countries in East Asia, South Korea has for several decades suffered a serious degradation of the
40 atmospheric environment, especially from severe cases of haze (H. C. Kim et al., 2017a). While high concentrations
41 of particulate matter have drawn strong public attention (K. Lee et al., 2020), rising concern has been paid to
42 surface ozone concentration (Kim et al., 2019), which has significantly increased in recent years. The puzzle of
43 surface ozone concentration in South Korea lies in its enigmatic long-term increase. Daily maximum eight-hour
44 moving average ozone concentrations (hereafter MDA8 ozone), a standard ozone metric of the U.S. EPA's National
45 Ambient Air Quality Standards, increased in Korea from 38.3 ppb in 2001 to 51.9 ppb in 2017, nearly 1 ppb per

46 year, during warm seasons (April to September) (**Figure S1**). This increase has caused much interest in the research
47 community and among policymakers.

48 There is no consensus explanation for such an increase in ozone in South Korea. Several speculative reasons
49 include (1) changes in NO_x emissions (Seo et al., 2014); (2) long-range transport, especially from China (Oh et al.,
50 2010); (3) changes in chemical regime (Bae et al., 2020); (4) stratospheric intrusion (Itahashi et al., 2020; Shin et al.,
51 2020); and (5) changes in meteorological condition. Until the early 2000s, increased ozone was usually explained as
52 a result of the rapid economic growth in East Asia and eventual corresponding increase in anthropogenic ozone
53 precursors, especially NO_x emissions. Later, however, ozone continued to increase, perplexingly, even as recently
54 reported surface and space observations suggest a decrease in NO₂ concentrations over East Asian countries, likely
55 due to more strict regulation (Duncan et al., 2016; Krotkov et al., 2016).

56 Several researchers have suggested that a change of chemical regime over Korea could explain the ozone increase.
57 Surface ozone is determined by the chemical characteristics of the response of tropospheric ozone to its
58 precursors, namely Ozone–NO_x–VOCs chemistry. Under a so-called NO_x-saturated regime, usually in large cities
59 with high NO_x emissions and low VOCs emissions, ozone responds positively to changes in VOCs and negatively to
60 changes in NO_x emissions. On the other hand, ozone increases with increasing NO_x and is insensitive to changes in
61 VOCs under a NO_x-sensitive regime, which occurs mostly in rural areas (Cohan et al., 2005; Sillman, 1999). This
62 chemical regime has been used to explain the increase in surface ozone concentrations in Japan and Taiwan in the
63 early 2000s. Recently, Bae et al. (2020) demonstrated the responses of surface ozone in South Korea using
64 adjusted NO_x emissions based on satellite observations (Bae et al., 2020). Showing negative ozone–NO_x
65 correlation, they suggested that the Seoul Metropolitan Area, South Korea is under a NO_x-saturated chemical
66 regime and that recent efforts to reduce NO_x emissions may have caused surface ozone to increase. However, this
67 explanation is insufficient to describe the long-term increase, since it remains to be determined whether and when
68 the chemical regime had changed. Hence, explaining the ozone increase due to the NO_x emission increase (in the
69 1980s and 1990s) as well as the NO_x emission decrease (in the 2000s) could be paradoxical.

70 Increased surface ozone has been reported in the northern hemisphere (Cooper et al., 2012; Mickley et al., 2004).
71 Allen et al. (2012) stated that atmospheric heating from black carbon and tropospheric ozone has generated a
72 poleward shift of the tropospheric jet, thereby relocating the main division between the tropical and temperature
73 air masses. Parrish et al. (2014) compared models and observations to reproduce the long-term increase in
74 tropospheric ozone. East Asia has one of the strongest increases in tropospheric ozone concentration based on
75 observations from 1970 to 2009 (Allen et al., 2012) or 2000 to 2014 (Chang et al., 2017). Several studies have
76 attributed the increased surface ozone over China to meteorological variations (Lu et al., 2019; Sun et al., 2019). Li
77 et al. (2019), on the other hand, claimed that ozone trends in the North China Plain from 2013 to 2017 were
78 mainly due to decreased PM_{2.5} concentration, which slowed the aerosol sink of hydroperoxy (HO₂) radicals and
79 accelerated ozone production.

80 Since this increase remains mysterious, we further explore the impact of weather. The influence of synoptic-scale
81 weather on regional air quality has attracted rising interest. Regional and local air quality are affected not only by
82 local precursor emissions but also by meteorological conditions, such as temperature, humidity, wind speed,
83 radiation, and the boundary layer. Changes in meteorological conditions, such as higher temperature, can enhance
84 chemical reactions and increase the release of biogenic emissions. Relative humidity and cloud coverage indicate
85 surface radiances that affect the rate of photolysis. Mixing depth is a key factor in diluting or accumulating
86 pollutants and their precursors. The transport of pollutants and precursors is also controlled by the local and
87 regional wind fields. Synoptic meteorology envelopes all these conditions; a change of synoptic weather pattern is
88 accompanied by dramatic change in these parameters. Therefore, understanding the relationship between
89 synoptic weather and air pollution will help assess the contribution of meteorology and climate to regional air
90 quality (Beaver and Palazoglu, 2009; Chen et al., 2008; Cheng et al., 2007; Liao et al., 2020; Pearce et al., 2011;
91 Triantafyllou, 2001).

92 Weather types are usually classified based on characteristics of varying types of air mass. Spatial Synoptic
93 Classification (SSC; <http://sheridan.geog.kent.edu/ssc.html>) (Sheridan, 2002) is one of methods that provide a daily
94 synoptic weather classification product. Since its initial suggestion (KALKSTEIN et al., 1996), the SSC has a rich
95 legacy in applications for many topics and many regions around the world, including South Korea, and in studies of

96 weather, climate, pollution, and health impacts. Since the SSC mainly uses the thermal properties of an air mass, it
97 has been used to investigate many extreme heat waves and the related epidemiology and the construction of
98 warning systems (Dixon et al., 2016; Hondula et al., 2014).

99 In South Korea, Kalkstein et al. (2011) developed a national heat-health warning system in collaboration with the
100 Korea Meteorological Administration. Kim (2019) used the SSC in South Korea to demonstrate how synoptic
101 weather impacts topics of epidemiological study. Since many of these studies have focused on the case of extreme
102 heat, they concluded that the occurrence of high temperature air masses (i.e., DT and MT; see Section 2.1) are
103 important to public health. Kim and Yum (2010) used synoptic classification to study the local and synoptic
104 characteristics of the fogs that have formed over Incheon International Airport on the west coast of Korea. Kim et
105 al. (2016) discussed the association of new particle formation according to the displacement of synoptic weather
106 systems. The SSC has also been used in air-quality studies in South Korea, especially those concerning ozone
107 (Cakmak et al., 2016; Hanna et al., 2011; Kim et al., 2014) and PM_{2.5} (Cakmak et al., 2018, 2016; Liu et al., 2017).

108 In this study, we aim to investigate the relationship between synoptic weather patterns and surface ozone
109 concentration over South Korea. Following the approaches of Kim et al. (2014), we explore several topics: (1)
110 determining the dominant synoptic weather type for high ozone occurrence, (2) estimating the efficiency of high
111 ozone occurrence, and (3) examining the implications of long-term variations in synoptic weather types for
112 regional air quality. The remainder of this paper is structured as follows. Section 2 explains the data and
113 methodology. Section 3 presents analyses on the characteristics of synoptic weather and surface ozone, as well as
114 their long-term variation. Section 4 concludes.

115 2. Data and Methodology

116 2.1. SSC

117 Synoptic weather includes meteorological phenomena that happen on a horizontal length scale of the order of
118 1000 kilometers or more. The daily weather types on the synoptic scale control many meteorological conditions
119 that are critical in the formation, dispersion, and transport of pollutants. The SSC, a clustering scheme for synoptic
120 weather patterns, has been developed as an analytical tool that can be applied to many natural and socioeconomic
121 issues, including health impacts (Hondula et al., 2014; Lee et al., 2012; Vanos et al., 2014), air pollution (Hebber
122 and Cakmak, 2015; Hu et al., 2010; Kim et al., 2018; Sheridan et al., 2008; Sullivan et al., 2015), vegetation
123 production, and past and future variations in climate (Bentley et al., 2010; Chow and Svoma, 2011; Hondula and
124 Davis, 2011; Sheridan, 2003). The SSC has been used for global applications, in North America (Delavau et al., 2015;
125 Dyer and Mote, 2007; Liu et al., 2013), Europe (Bower et al., 2007; Makra et al., 2015), and East Asia (Cakmak et
126 al., 2016; Hanna et al., 2011; Kim et al., 2014).

127 For the present study, we obtained daily SSC classifications at 17 airport meteorological monitoring sites in South
128 directly from the SSC homepage (<http://sheridan.geog.kent.edu/ssc.html>). The SSC utilizes synoptic-scale, daily
129 classifications of different types of air masses based on the thermal and moisture characteristics of each type.
130 Seven meteorological variables classify each day's synoptic pattern: afternoon surface temperature, dew point,
131 dew point depression, wind speed, wind direction, cloud cover, and diurnal temperature range. The SSC algorithm
132 compares the surface observations of each variable with so-called "seed days" that are representative of various
133 air masses for a given day and location. Since seed characteristics vary by time and location, the SSC provides a
134 relative classification system (Sheridan, 2002).

135 The SSC includes nine synoptic weather types, six main categories and three additional or transitional categories.
136 DP (dry polar) denotes an air mass originating from polar regions and is usually associated with low temperature
137 and low humidity. It is synonymous with the traditional cP (continental polar) air mass classification. DM (dry
138 moderate) air mass has mild and dry characteristics and is often found with zonal flow in the middle latitudes,
139 especially on the leeward side of mountains. DT (dry tropical) is the hottest and driest air mass, similar to the traditional
140 cT (continental tropical) air mass. MP (moist polar) air is humid and cool like the traditional mP air mass type, and
141 MM (moist moderate) is assigned in the case of considerably warmer and more humid air. MT (moist tropical) air is
142 warm and very humid (i.e., the traditional mT air mass), often found in the warm sector of mid-latitude cyclones.
143 Extreme cases of the MT type are separated into MTP (moist tropical plus) and MTDP (moist tropical double-plus).
144 Most MTP or MTDP cases happen during summer. Days transitioning between one weather type and another,
145 considered to be TR (transitional), are characterized by large shifts in pressure, dew point, and wind pattern. The

146 list and geographical coverage of the meteorological stations used in the study are shown in **Table S1** and **Figure**
147 **S2**.

148 **2.2. Observations**

149 Hourly observations of surface ozone concentrations from 2001 to 2017 were collected from AirKorea
150 (<http://www.airkorea.or.kr/>). Data from 306 surface monitoring sites (251 urban, 38 roadside, and 17 background
151 sites) were selected after screening their data quality and availability. Meteorological observations for
152 temperature, dew point, relative humidity, wind speed, cloud fraction, and surface pressure were collected from
153 the surface monitoring sites operated by the Korea Meteorological Administration (KMA; available from the data
154 archive portal at <http://data.kma.go.kr/>). Surface ozone concentrations and meteorological variables were paired
155 with the SSC by assigning the closest SSC site locations to determine daily SSC weather.

156 **3. Results**

157 **3.1. Synoptic Weather in South Korea**

158 South Korea has distinctive seasonal variations in weather, as the country is affected by both continental and
159 maritime air masses. South Korea is in the Asian monsoon regime, affected by cold air masses from the Asian
160 continent during winter and warm and moist air masses of tropical origin during summer. In traditional air mass
161 classification, several air masses affect South Korea: the Siberian air mass (cP), Okhotsk sea air mass (mP), North
162 Pacific air mass (mT), Equatorial air mass (cT), and Yangtze River air mass. In spring, the Yangtze River air mass is
163 dominant, with migratory cyclones and anticyclones. The routine passage of migratory systems—also known as
164 *three cold days and four warm days* in Korean idiom—and the emergence of cases of Asian dust characterize the
165 Korean spring. In early summer, the Okhotsk sea and North Pacific air masses are strong, often causing a rainy
166 season when the strengths of two air masses are balanced. In the summer, the North Pacific air mass is dominant;
167 in the winter, the Siberian air mass is dominant, with prevailing northwesterly wind patterns.

168 These seasonal variations are reflected in the seasonal SSC patterns. **Figure 1** shows seasonal variation in the SSC
169 as determined from 17 meteorological monitoring sites in South Korea. As expected, the general synoptic weather
170 patterns in South Korea are clearly seasonal. DM is a common weather type in all seasons except July and August
171 when the East Asian summer monsoon is dominant. During the cold season, polar types (DP and MP) prevail as the
172 strong high-pressure system over Siberia (the Siberian High) often extends, and the transboundary movement of
173 the synoptic system affects South Korea. Spring is characterized by consistent passages of transboundary systems,
174 both cyclonic and anticyclonic. Interestingly, from March to May, DT has a remarkable presence during spring.
175 Moist types (MM and MT) are dominant in summer. The start of the summer season happens alongside the
176 summer monsoon season. In this season, the wind flow pattern also changes, and marine flow patterns
177 characterize the humidity of the airshed.

178 **Table 1** summarizes the frequencies of each type of SSC occurring over South Korea from 2001 to 2017. Annually,
179 DM is the dominant type, accounting for 32.8% of synoptic patterns, followed by MM (15.7%) and MT (13%,
180 including MTP and MTDP). DT and MP happen rarely, with frequencies of 5.9% and 3.7%, respectively. SSC types
181 display clear seasonal variation, as the displacement of air masses is strongly affected by the development of
182 monsoons. During the monsoon season, flow patterns change dramatically because of the different heat capacities
183 of ocean and land.

184 The meteorological characteristics of each type of SSC are summarized in **Table 2**. As expected from the
185 classification method, each type represents distinctive thermal and moisture properties. Warm air masses (e.g.,
186 DT, MT, MTP, and MTDP) have higher temperatures, while dry air masses (e.g., DM, DP, and DT) have drier and less
187 cloudy conditions. Notably, the DT type has the lowest cloud fraction (37.6%) and wind speed (2.01 m/s), providing
188 stagnant conditions with high photolysis potential.

189 **3.2. SSC and High Ozone Occurrence**

190 Next, we analyze the connection between the occurrence of high ozone and synoptic weather patterns. **Figure 2**
191 demonstrates the extent to which the occurrence of surface ozone differs by SSC weather type. We count the
192 number of occurrences in each 1 ppb ozone bin for each SSC type. A total of 105,553 data points are used for the
193 analyses, and **Figure 2a** shows the normalized distribution of MDA8 ozone for each SSC type. Summing the

194 occurrences for all eight SSC types yields 100%. While DM occurs the most frequently throughout the whole
195 concentration range, with a mean value of 38 ppb, the distribution of DT, which occurs less frequently, is skewed
196 toward higher ozone concentrations, with a mean value of 57 ppb. The other types also show distinctive statistical
197 characteristics. **Table 2** also presents statistics of MDA8 ozone concentrations for each SSC type.

198 The link between SSC type and ozone level is clearly presented in **Figure 2b**, which shows the occurrence frequency
199 of each SSC type for 1 ppb bins up to 100 ppb. In most cases, DP is associated with lower ozone concentrations,
200 showing seasonal dependency. MM, on the other hand, happens more during summer but is strongly associated
201 with lower ozone, implying that moist conditions (e.g., more cloud) are not favorable for ozone production. For
202 high ozone concentrations, DT, DM, and MT are the three dominant types, accounting for more than 80% of all
203 events exceeding 80 ppb. DT and MT, both characterized by high temperatures, are associated with high ozone
204 concentrations, but they differ in terms of the efficiency in the high concentration ozone occurrence. A large
205 proportion of high-ozone events happen during the DT synoptic type (dry with high temperatures). This reconfirms
206 that sunlight is critical in ozone formation. Forty-four percent of 100 ppb or higher ozone events happened in the
207 DT type (compared with 25% in DM and 20% in MT), so we conclude that the DT synoptic type has the highest
208 efficiency of high concentration ozone occurrence.

209 The ozone-production mechanism is usually associated with warmer conditions. High temperature directly
210 enhances chemical processes and biogenic emissions and is also associated with less cloudy conditions, which yield
211 stronger photochemistry. However, with this current method of analysis, we cannot totally exclude the potential
212 contribution of other factors. For example, DT happens frequently during spring, coincident with the dominant
213 westerly flows over South Korea. Therefore, the efficiency of the DT type for high ozone occurrence may include
214 the transport of ozone and/or its precursors from Chinese emission sources.

215 Separating the impacts between local formation and regional transport would be valuable information for regional
216 chemistry and emissions control policy. Although we cannot separate these factors quantitatively at this point, we
217 can explore the characteristics of the high concentration ozone occurring in the region. First, **Figure 3** shows the
218 diurnal variations in hourly ozone concentrations according to each SSC weather type. Consistent with our
219 previous analysis, the diurnal variations in surface ozone concentrations during the warm season show distinctive
220 features for each SSC type. As expected, DT is associated with the highest level of surface ozone during the warm
221 season (i.e., April to September), followed by DM and MT group (MTP and MTDP). Nighttime (including early
222 morning) ozone concentrations in DT are not specifically high compared with those of the other SSC types,
223 suggesting no evidence of elevated background concentrations. During DT synoptic weather, ozone concentration
224 increases by 47.7 ppb from morning (16.7 ppb) to the afternoon peak (64.4 ppb), showing a strong capability of
225 ozone formation. The lowest increase, 9.5 ppb, happens in the MP weather type, which characterizes humid and
226 cold air masses. High daily peak concentrations are mostly associated with a rapid daytime increase, suggesting the
227 role of local formation.

228 Second, the transport pathways for each SSC type are also analyzed. We conduct five-year (2012 to 2016)
229 backward trajectory simulations using the NOAA HYSPLIT model (Stein et al., 2015). The daily trajectory
230 simulations reaching the GMP monitor (Gimpo International Airport at a 100-m altitude at midday local time) are
231 classified based on their spatial variances (Stunder, 1996). **Figure 4a** show the distributions of the clustered
232 trajectories of the DT synoptic type in the warm season (April – September) during 2012–2016. Four cluster
233 numbers are chosen based on the change in total spatial variance (**Figure 4b**). Except a small number of long-range
234 transport cases (7.5%), most trajectories originate from nearby locations, showing a weak wind field during the DT
235 weather type; 55% of trajectories are from Chinese sources (45.8% from northern China and 9.2% from southern
236 China); and 35.8% trajectories from the East Sea (i.e., easterly flow). For these clustered trajectory groups, we
237 calculate the mean MDA8 O₃ concentrations (137 sites in the Seoul metropolitan area). The results show no clear
238 dependency of ozone concentration on flow pattern direction; the highest concentration is from southern Chinese
239 sources (63.2 ppb) and the lowest is from the long-range case (55.0 ppb) (**Figure 4c**). This also implies the likely
240 role of local formation rather than transport from outside.

241 3.3. Long-Term Variation in SSC Types

242 Having demonstrated that the production of surface ozone is affected by synoptic weather patterns, we further
243 investigated the long-term variation in SSC types. As the previous analysis showed, certain synoptic weather

244 patterns are tightly associated with the occurrence of high ozone concentration. This clearly implies that changes
245 in synoptic weather can be directly associated with the occurrence of pollution, showing the crucial connections
246 between pollution and weather and between pollution and climate.

247 To test this, we further investigate the long-term variation in the occurrence frequency of synoptic patterns over
248 the past 50 years. **Figure 5** shows a time series of SSC interannual variation from 1965 to 2017. There are several
249 noticeable changes in the occurrence of SSC types, implying that the South Korean region has been affected by
250 long-term changes in climate. Two noticeable variations are the increasing trend in DT and MT and the decreasing
251 trend in MP, DP, and MM. DT occurred with an approximately 2% frequency in the 1960s and 1970s but increased
252 up to an 8% frequency in the past two decades. The increase in DT appears to become especially strong after 2000.

253 Evidently, the long-term variation in SSC types in South Korea is associated with changing climatological
254 characteristics, with an increasing trend in tropical air masses and a declining trend in polar air masses. This is
255 consistent with the findings from the previous literature based on long-term observations (Chung et al., 2004;
256 Chung and Yoon, 2000; H.-S. S. Kim et al., 2016; Yun et al., 2012) and models (Jeung et al., 2019; Kwon et al., 2007;
257 Yun et al., 2012). Long-term reanalysis datasets also confirm the consistent result in the changes in meteorological
258 variations over South Korea (**Figure 6**). We analyze the long-term variations in 2-m temperature and relative
259 humidity over Korea (i.e. 126°E–130°E, 34°N–39°N) using six global reanalysis data sets: JRA-55 (1958–2017),
260 MERRA2 (1980–2017), ERA5 (1979–2017), ERA_interim (1979–2017), NCEP/NCAR R1 (1958–2017), and
261 NCEP/NCAR R2 (1979–2017). All the reanalysis data show consistent trends, namely, increasing 2-m temperature
262 and decreasing relative humidity, which characterize the meteorological properties in DT. This change in DT may
263 be related to climate change and could imply long-term changes in air quality. Recent studies have suggested that
264 the increased temperature owing to climate change could weaken the meridional thermal gradient between the
265 equator and poles, causing more stagnant conditions in the region and resulting in deteriorated regional air quality
266 (H. C. Kim et al., 2017b; Mickley, 2004). The recent study by Lee et al. (2020) used CMIP5 single-forcing
267 experiments to demonstrate that climate change can degrade regional air quality, by increasing static stability and
268 reducing wind speed.

269 3.4. Ozone Sensitivity to Changes in SSC Types

270 In this section, we estimate how surface-ozone distribution has changed as a result of the increased occurrence of
271 the DT type. Quantifying the changes in surface ozone concentration as a response to incremental changes in the
272 occurrence of the DT type helps explain the relationship between weather and pollution in the region. Although
273 the DT type occurs less frequently than the other types such as DM or MM, as described in the previous section, it
274 contributes to high ozone production and its frequency has greatly increased in recent decades.

275 A complete estimate of the effect of changes in synoptic patterns is not easy to obtain, considering the presence of
276 more complicated effects, such as the transport patterns of precursor emissions. However, the sensitivity of ozone
277 production to SSC changes is testable by making two simple assumptions: (1) total occurrence counts are constant
278 and (2) the shape of the ozone distribution for each SSC type is consistent.

279 Beginning from the probability distribution in **Figure 2a**, we change the occurrence frequency of the DT type while
280 preserving the total count of occurrences:

$$\begin{aligned} 281 \quad n_{total} &= n_{DT} + n_{non-DT} \\ 282 \quad &= a \cdot n_{DT} + b \cdot n_{non-DT} \end{aligned}$$

283 where n_{DT} and n_{non-DT} indicate the total ozone distribution for the DT type and seven other types, respectively,
284 and a and b are adjustment coefficients for the sensitivity test. In this case, increasing the occurrence of DT types
285 by applying $a = 2, 3$, the adjustment coefficient for the other types, b , will decrease, and we can specify its value if
286 the total count, n_{total} , is preserved.

287 **Figure 7** demonstrates how this sensitivity test works. We obtained the non-DT coefficient $b = 0.934, 0.868$ when
288 DT frequency is doubled or tripled (e.g., $a = 2, 3$) with the total count preserved. Since the DT type only account for
289 a small proportion of the total distribution, doubling the DT distribution results in a 6.5% decrease in the other SSC
290 types.

291 Making these adjustments, the general distributions of MDA8 ozone show noticeable changes in both average and
292 peak values. The averages of MDA8 ozone are increased by 3.5% and 7.5% for $a = 2, 3$, respectively. Moreover, the
293 high ozone-production efficiency of the DT type really alters the higher concentration levels. **Figure 7b** presents
294 the change in the MDA8 ozone distribution after doubling or tripling the prevalence of the DT type. At lower
295 concentrations, MDA8 ozone decreases by around 5% or 10% for doubling and tripling, respectively. However,
296 because of the highly skewed distribution of DT ozone, at higher concentration levels, MDA8 ozone increases. A
297 transition happens near 45 ppb in both cases; the occurrence of 80 ppb ozone increases by 25.2% with doubled DT
298 and by over 50.4% with tripled DT frequencies (31.7% and 63.3% for >80 ppb, cumulatively). Higher-level ozone
299 increases quickly—by almost 80%—when $a = 3$ is applied. This is a good example of the high efficiency of the DT
300 type in producing surface ozone; the DT type thus provides very favorable weather conditions for ozone
301 production.

302 We do not attribute all the increase in this sensitivity test to the increased prevalence of DT. However, DT clearly
303 provides favorable conditions for high ozone production. In addition, it should be noted that the SSC impact seems
304 to be meteorological but does not include the potential impacts from the changes in transport patterns resulting
305 from each SSC type. As DT represents a typical transport pathway from China, a more detailed investigation of
306 transport impacts is therefore warranted.

307 **4. Conclusion**

308 In this study, we investigated the association between weather and pollution using surface ozone and SSC data
309 over South Korea. We used the synoptic weather classification data to relate meteorological conditions to surface
310 ozone concentrations. The analyses of daily maximum eight-hour ozone revealed that DM, MT, and DT are the
311 most common synoptic weather types associated with episodes of high ozone concentration. Among these, the DT
312 type shows the highest correlation with such episodes, implying that air masses' thermal and moisture
313 characteristics are associated with the formation of high ozone concentrations.

314 We further explored the long-term variation in synoptic weather types, with results demonstrating that the DT
315 type has occurred more frequently in recent years. This increased pattern makes sense given changes in typical
316 weather in South Korea. Several reports have suggested that the climatological characteristics in South Korea are
317 warming in general.

318 The findings from this study are summarized as follows:

- 319 1) Surface ozone distributions show distinctive characteristics for each synoptic weather pattern.
- 320 2) The occurrence of the DT type is strongly tied to the occurrence of high ozone concentrations. With MDA8
321 over 100 ppb, the frequency of the DT type is over 44%.
- 322 3) The long-term variation in the SSC weather types shows clear long-term trends in several of the SSC types.
323 In particular, the DT type has increased in prevalence over the past 50 years. This further implies that any
324 change in the occurrence of DT weather types in the anticipated climate change scenario could affect the
325 development of regional air quality for all regions in the future.
- 326 4) We estimated the extent to which the change in the prevalence of the DT type affects the total
327 distribution of surface ozone level and occurrence of high ozone levels. Sensitivity tests revealed that
328 when the DT type doubles or triples in occurrence, mean ozone increases by 3% and 7%, respectively. For
329 high ozone, this effect is even more significant.

330 Based on these findings, we conclude that changes in meteorological condition could have led to the changes in
331 surface ozone concentration trends over South Korea. Notably, we do not exclude the impact of emissions changes
332 on the current ozone trend. The currently observed increase in surface ozone concentrations in South Korea could
333 combine impacts from changes in anthropogenic emission with meteorological conditions. Clearly, the direction of
334 climate change in the region favors conditions for high ozone concentration. In summary, changes in weather type
335 can play an important role in regional air quality. While limited, the findings of this study contribute to our
336 understanding of how long-term and large-scale changes in climate are linked to short-term and local-scale
337 pollution events.

338 **5. References**

- 339 Allen, R.J., Sherwood, S.C., Norris, J.R., Zender, C.S., 2012. Recent Northern Hemisphere tropical expansion
340 primarily driven by black carbon and tropospheric ozone. *Nature* 485, 350–354.
341 <https://doi.org/10.1038/nature11097>
- 342 Bae, C., Kim, B.-U., Kim, H.C., Kim, S., 2018. Quantitative Assessment on Contributions of Foreign NO_x and VOC
343 Emission to Ozone Concentrations over Gwangyang Bay with CMAQ-HDDM Simulations. *J. Korean Soc.*
344 *Atmos. Environ.* 34, 708–726. <https://doi.org/10.5572/KOSAE.2018.34.5.708>
- 345 Bae, C., Kim, H.C., Kim, B.-U., Kim, S., 2020. Surface ozone response to satellite-constrained NO_x emission
346 adjustments and its implications. *Environ. Pollut.* 258, 113469.
347 <https://doi.org/10.1016/j.envpol.2019.113469>
- 348 Beaver, S., Palazoglu, A., 2009. Influence of synoptic and mesoscale meteorology on ozone pollution potential for
349 San Joaquin Valley of California. *Atmos. Environ.* 43, 1779–1788.
350 <https://doi.org/10.1016/j.atmosenv.2008.12.034>
- 351 Bentley, M.L., Ashley, W.S., Stallins, J.A., 2010. Climatological radar delineation of urban convection for Atlanta,
352 Georgia. *Int. J. Climatol.* 30, 1589–1594. <https://doi.org/10.1002/joc.2020>
- 353 Bloomer, B.J., Stehr, J.W., Piety, C.A., Salawitch, R.J., Dickerson, R.R., 2009. Observed relationships of ozone air
354 pollution with temperature and emissions. *Geophys. Res. Lett.* 36, L09803.
355 <https://doi.org/10.1029/2009GL037308>
- 356 Bower, D., McGregor, G.R., Hannah, D.M., Sheridan, S.C., 2007. Development of a spatial synoptic classification
357 scheme for western Europe. *Int. J. Climatol.* 27, 2017–2040. <https://doi.org/10.1002/joc.1501>
- 358 Cakmak, S., Hebbern, C., Pinault, L., Lavigne, E., Vanos, J., Crouse, D.L., Tjepkema, M., 2018. Associations between
359 long-term PM_{2.5} and ozone exposure and mortality in the Canadian Census Health and Environment Cohort
360 (CANCHEC), by spatial synoptic classification zone. *Environ. Int.* 111, 200–211.
361 <https://doi.org/10.1016/j.envint.2017.11.030>
- 362 Cakmak, S., Hebbern, C., Vanos, J., Crouse, D.L., Burnett, R., 2016. Ozone exposure and cardiovascular-related
363 mortality in the Canadian Census Health and Environment Cohort (CANCHEC) by spatial synoptic
364 classification zone. *Environ. Pollut.* 214, 589–599. <https://doi.org/10.1016/j.envpol.2016.04.067>
- 365 Camalier, L., Cox, W., Dolwick, P., 2007. The effects of meteorology on ozone in urban areas and their use in
366 assessing ozone trends. *Atmos. Environ.* 41, 7127–7137. <https://doi.org/10.1016/j.atmosenv.2007.04.061>
- 367 Chang, K.-L., Petropavlovskikh, I., Copper, O.R., Schultz, M.G., Wang, T., 2017. Regional trend analysis of surface
368 ozone observations from monitoring networks in eastern North America, Europe and East Asia. *Elem Sci Anth*
369 5, 50. <https://doi.org/10.1525/elementa.243>
- 370 Chen, Z.H., Cheng, S.Y., Li, J.B., Guo, X.R., Wang, W.H., Chen, D.S., 2008. Relationship between atmospheric
371 pollution processes and synoptic pressure patterns in northern China. *Atmos. Environ.* 42, 6078–6087.
372 <https://doi.org/10.1016/j.atmosenv.2008.03.043>
- 373 Cheng, C.S., Campbell, M., Li, Q., Li, G., Auld, H., Day, N., Pengelly, D., Gingrich, S., Yap, D., 2007. A Synoptic
374 Climatological Approach to Assess Climatic Impact on Air Quality in South-central Canada. Part II: Future
375 Estimates. *Water. Air. Soil Pollut.* 182, 117–130. <https://doi.org/10.1007/s11270-006-9326-4>
- 376 Chow, W.T.L., Svoma, B.M., 2011. Analyses of Nocturnal Temperature Cooling-Rate Response to Historical Local-
377 Scale Urban Land-Use/Land Cover Change. *J. Appl. Meteorol. Climatol.* 50, 1872–1883.
378 <https://doi.org/10.1175/JAMC-D-10-05014.1>
- 379 Chung, Y.-S., Yoon, M.-B., Kim, H.-S., 2004. On Climate Variations and Changes Observed in South Korea. *Clim.*
380 *Change* 66, 151–161. <https://doi.org/10.1023/B:CLIM.0000043141.54763.f8>
- 381 Chung, Y.S., Yoon, M.B., 2000. Interpretation of recent temperature and precipitation trends observed in Korea.

382 Theor. Appl. Climatol. 67, 171–180. <https://doi.org/10.1007/s007040070006>

383 Cohan, D.S., Hakami, A., Hu, Y., Russell, A.G., 2005. Nonlinear response of ozone to emissions: Source
384 apportionment and sensitivity analysis. Environ. Sci. Technol. 39, 6739–6748.
385 <https://doi.org/10.1021/es048664m>

386 Cooper, O.R., Gao, R.-S., Tarasick, D., Leblanc, T., Sweeney, C., 2012. Long-term ozone trends at rural ozone
387 monitoring sites across the United States, 1990-2010. J. Geophys. Res. Atmos. 117, n/a-n/a.
388 <https://doi.org/10.1029/2012JD018261>

389 Delavau, C., Chun, K.P., Stadnyk, T., Birks, S.J., Welker, J.M., 2015. North American precipitation isotope ($\delta^{18}O$)
390 zones revealed in time series modeling across Canada and northern United States. Water Resour. Res. 51,
391 1284–1299. <https://doi.org/10.1002/2014WR015687>

392 Dixon, P.G., Allen, M., Gosling, S.N., Hondula, D.M., Ingole, V., Lucas, R., Vanos, J., 2016. Perspectives on the
393 Synoptic Climate Classification and its Role in Interdisciplinary Research. Geogr. Compass 10, 147–164.
394 <https://doi.org/10.1111/gec3.12264>

395 Duncan, B.N., Lamsal, L.N., Thompson, A.M., Yoshida, Y., Lu, Z., Streets, D.G., Hurwitz, M.M., Pickering, K.E., 2016.
396 A space-based, high-resolution view of notable changes in urban NO_x pollution around the world (2005-
397 2014). J. Geophys. Res. Atmos. 121, 976–996. <https://doi.org/10.1002/2015JD024121>

398 Dyer, J.L., Mote, T.L., 2007. Trends in snow ablation over North America. Int. J. Climatol. 27, 739–748.
399 <https://doi.org/10.1002/joc.1426>

400 Hanna, A.F., Yeatts, K.B., Xiu, A., Zhu, Z., Smith, R.L., Davis, N.N., Talgo, K.D., Arora, G., Robinson, P.J., Meng, Q.,
401 Pinto, J.P., 2011. Associations between ozone and morbidity using the Spatial Synoptic Classification system.
402 Environ. Health 10, 49. <https://doi.org/10.1186/1476-069X-10-49>

403 Hebborn, C., Cakmak, S., 2015. Synoptic weather types and aeroallergens modify the effect of air pollution on
404 hospitalisations for asthma hospitalisations in Canadian cities. Environ. Pollut. 204, 9–16.
405 <https://doi.org/10.1016/j.envpol.2015.04.010>

406 Hondula, D.M., Davis, R.E., 2011. Climatology of winter transition days for the contiguous USA, 1951–2007. Theor.
407 Appl. Climatol. 103, 27–37. <https://doi.org/10.1007/s00704-010-0278-7>

408 Hondula, D.M., Vanos, J.K., Gosling, S.N., 2014. The SSC: a decade of climate–health research and future directions.
409 Int. J. Biometeorol. 58, 109–120. <https://doi.org/10.1007/s00484-012-0619-6>

410 Hu, Y., Chang, M.E., Russell, A.G., Odman, M.T., 2010. Using synoptic classification to evaluate an operational air
411 quality forecasting system in Atlanta. Atmos. Pollut. Res. 1, 280–287. <https://doi.org/10.5094/APR.2010.035>

412 Itahashi, S., Mathur, R., Hogrefe, C., Zhang, Y., 2020. Modeling stratospheric intrusion and trans-Pacific transport
413 on tropospheric ozone using hemispheric CMAQ during April 2010 – Part 1: Model evaluation and air mass
414 characterization for stratosphere–troposphere transport. Atmos. Chem. Phys. 20, 3373–3396.
415 <https://doi.org/10.5194/acp-20-3373-2020>

416 Jeung, S.J., Sung, J.H., Kim, B.S., 2019. Assessment of the Impacts of Climate Change on Climatic Zones over the
417 Korean Peninsula. Adv. Meteorol. 2019, 1–11. <https://doi.org/10.1155/2019/5418041>

418 KALKSTEIN, L.S., NICHOLS, M.C., BARTHEL, C.D., GREENE, J.S., 1996. A NEW SPATIAL SYNOPTIC CLASSIFICATION:
419 APPLICATION TO AIR-MASS ANALYSIS. Int. J. Climatol. 16, 983–1004. [https://doi.org/10.1002/\(SICI\)1097-0088\(199609\)16:9<983::AID-JOC61>3.0.CO;2-N](https://doi.org/10.1002/(SICI)1097-0088(199609)16:9<983::AID-JOC61>3.0.CO;2-N)

421 Kalkstein, L.S., Sheridan, S.C., Vanos, J.K., 2011. INSIGHTS INTO THE HEALTH IMPACTS OF SYNOPTIC-SCALE
422 CLIMATOLOGY IN TWO KOREAN CITIES : A RETROSPECTIVE ANALYSIS OF MORBIDITY.

423 Kim, B.-U., Kim, H.C., Kim, S., 2019. Review on Ozone Management in US and Recommendations for Domestic

424 Ozone Control. *J. Korean Soc. Atmos. Environ.* 35, 370–394. <https://doi.org/10.5572/kosae.2019.35.3.370>

425 Kim, C.K., Yum, S.S., 2010. Local meteorological and synoptic characteristics of fogs formed over Incheon
426 international airport in the west coast of Korea. *Adv. Atmos. Sci.* 27, 761–776.
427 <https://doi.org/10.1007/s00376-009-9090-7>

428 Kim, E., Kim, B.-U., Kim, H., Kim, S., 2017. The Variability of Ozone Sensitivity to Anthropogenic Emissions with
429 Biogenic Emissions Modeled by MEGAN and BEIS3. *Atmosphere (Basel)*. 8, 187.
430 <https://doi.org/10.3390/atmos8100187>

431 Kim, H.-S.S., Chung, Y.-S.S., Tans, P.P., Yoon, M.-B.B., 2016. Climatological variability of air temperature and
432 precipitation observed in South Korea for the last 50 years. *Air Qual. Atmos. Heal.* 9, 645–651.
433 <https://doi.org/10.1007/s11869-015-0366-z>

434 Kim, H.C., Choi, H., Ngan, F., Lee, P., Steyn, D., Mathur, R., 2014. Surface Ozone Variability in Synoptic Pattern
435 Perspectives, in: *Air Pollution Modeling and Its Application Xxiii*. pp. 551–556. https://doi.org/10.1007/978-3-319-04379-1_91

437 Kim, H.C., Kim, S., Kim, B.-U., Jin, C.-S., Hong, S., Park, R., Son, S.-W., Bae, C., Bae, M., Song, C.-K., Stein, A., 2017a.
438 Recent increase of surface particulate matter concentrations in the Seoul Metropolitan Area, Korea. *Sci. Rep.*
439 7, 4710. <https://doi.org/10.1038/s41598-017-05092-8>

440 Kim, H.C., Kim, S., Kim, B.-U., Jin, C.-S., Hong, S., Park, R., Son, S.-W., Bae, C., Bae, M., Song, C.-K., Stein, A., 2017b.
441 Recent increase of surface particulate matter concentrations in the Seoul Metropolitan Area, Korea. *Sci. Rep.*
442 7, 4710. <https://doi.org/10.1038/s41598-017-05092-8>

443 Kim, H.C.C., Lee, P., Ngan, F., Tang, Y., Yoo, H.L.L., Pan, L., 2015. Evaluation of modeled surface ozone biases as a
444 function of cloud cover fraction. *Geosci. Model Dev.* 8, 2959–2965. <https://doi.org/10.5194/gmd-8-2959-2015>

446 Kim, J., 2019. Particulate Matter Mortality Rates and Their Modification by Spatial Synoptic Classification. *Int. J.*
447 *Environ. Res. Public Health* 16, 1904. <https://doi.org/10.3390/ijerph16111904>

448 Kim, Y.-M., Kim, J., Jung, K., Eo, S., Ahn, K., 2018. The effects of particulate matter on atopic dermatitis symptoms
449 are influenced by weather type: Application of spatial synoptic classification (SSC). *Int. J. Hyg. Environ. Health*
450 221, 823–829. <https://doi.org/10.1016/j.ijheh.2018.05.006>

451 Kim, Y., Kim, S.-W., Yoon, S.-C., Park, J.-S., Lim, J.-H., Hong, J., Lim, H.-C., Ryu, J., Lee, C.-K., Heo, B.-H., 2016.
452 Characteristics of formation and growth of atmospheric nanoparticles observed at four regional background
453 sites in Korea. *Atmos. Res.* 168, 80–91. <https://doi.org/10.1016/j.atmosres.2015.08.020>

454 Krotkov, N. a., McLinden, C. a., Li, C., Lamsal, L.N., Celarier, E. a., Marchenko, S. V., Swartz, W.H., Bucsela, E.J.,
455 Joiner, J., Duncan, B.N., Boersma, K.F., Veefkind, J.P., Levelt, P.F., Fioletov, V.E., Dickerson, R.R., He, H., Lu, Z.,
456 Streets, D.G., 2016. Aura OMI observations of regional SO₂ and NO₂ pollution changes from 2005 to 2015.
457 *Atmos. Chem. Phys.* 16, 4605–4629. <https://doi.org/10.5194/acp-16-4605-2016>

458 Kwon, Y.-A., Kwon, W.-T., Boo, K.-O., Choi, Y., 2007. Future Projections on Subtropical Climate Regions over South
459 Korea Using SRES A1B Data.

460 Lee, C.C., Sheridan, S.C., Lin, S., 2012. Relating Weather Types to Asthma-Related Hospital Admissions in New York
461 State. *Ecohealth* 9, 427–439. <https://doi.org/10.1007/s10393-012-0803-5>

462 Lee, D., Simon Wang, S.Y., Zhao, L., Kim, H.C., Kim, K., Yoon, J.-H., 2020. Long-term increase in atmospheric
463 stagnant conditions over northeast Asia and the role of greenhouse gases-driven warming. *Atmos. Environ.*
464 117772. <https://doi.org/10.1016/j.atmosenv.2020.117772>

465 Lee, K., Park, Y., Han, S.-P., Kim, H.C., 2020. The Alerting Effect from Rising Public Awareness of Air Quality on the
466 Outdoor Activities of Megacity Residents. *Sustainability* 12, 820. <https://doi.org/10.3390/su12030820>

- 467 Li, K., Jacob, D.J., Liao, H., Shen, L., Zhang, Q., Bates, K.H., 2019. Anthropogenic drivers of 2013–2017 trends in
468 summer surface ozone in China. *Proc. Natl. Acad. Sci.* 116, 422–427.
469 <https://doi.org/10.1073/pnas.1812168116>
- 470 Liao, W., Wu, L., Zhou, S., Wang, X., Chen, D., 2020. Impact of Synoptic Weather Types on Ground-Level Ozone
471 Concentrations in Guangzhou, China. *Asia-Pacific J. Atmos. Sci.* <https://doi.org/10.1007/s13143-020-00186-2>
- 472 Liu, Y., Zhao, N., Vanos, J.K., Cao, G., 2017. Effects of synoptic weather on ground-level PM 2.5 concentrations in
473 the United States. *Atmos. Environ.* 148, 297–305. <https://doi.org/10.1016/j.atmosenv.2016.10.052>
- 474 Liu, Z., Bowen, G.J., Welker, J.M., Yoshimura, K., 2013. Winter precipitation isotope slopes of the contiguous USA
475 and their relationship to the Pacific/North American (PNA) pattern. *Clim. Dyn.* 41, 403–420.
476 <https://doi.org/10.1007/s00382-012-1548-0>
- 477 Lu, X., Zhang, L., Chen, Y., Zhou, M., Zheng, B., Li, K., Liu, Y., Lin, J., Fu, T.-M.M., Zhang, Q., 2019. Exploring 2016–
478 2017 surface ozone pollution over China: source contributions and meteorological influences. *Atmos. Chem.*
479 *Phys.* 19, 8339–8361. <https://doi.org/10.5194/acp-19-8339-2019>
- 480 Makra, L., Puskás, J., Matyasovszky, I., Csépe, Z., Lelovics, E., Bálint, B., Tusnády, G., 2015. Weather elements,
481 chemical air pollutants and airborne pollen influencing asthma emergency room visits in Szeged, Hungary:
482 performance of two objective weather classifications. *Int. J. Biometeorol.* 59, 1269–1289.
483 <https://doi.org/10.1007/s00484-014-0938-x>
- 484 Mickley, L.J., 2004. Effects of future climate change on regional air pollution episodes in the United States.
485 *Geophys. Res. Lett.* 31, L24103. <https://doi.org/10.1029/2004GL021216>
- 486 Mickley, L.J., Jacob, D.J., Field, B.D., 2004. Effects of future climate change on regional air pollution episodes in the
487 United States. *Geophys. Res. Lett.* 31, L24103. <https://doi.org/10.1029/2004GL021216>
- 488 Oh, I.-B., Kim, Y.-K., Hwang, M.-K., Kim, C.-H., Kim, S., Song, S.-K., 2010. Elevated Ozone Layers over the Seoul
489 Metropolitan Region in Korea: Evidence for Long-Range Ozone Transport from Eastern China and Its
490 Contribution to Surface Concentrations. *J. Appl. Meteorol. Climatol.* 49, 203–220.
491 <https://doi.org/10.1175/2009JAMC2213.1>
- 492 Parrish, D.D., Lamarque, J.-F., Naik, V., Horowitz, L., Shindell, D.T., Staehelin, J., Derwent, R., Cooper, O.R.,
493 Tanimoto, H., Volz-Thomas, A., Gilge, S., Scheel, H.-E., Steinbacher, M., Fröhlich, M., 2014. Long-term
494 changes in lower tropospheric baseline ozone concentrations: Comparing chemistry-climate models and
495 observations at northern midlatitudes. *J. Geophys. Res. Atmos.* 119, 5719–5736.
496 <https://doi.org/10.1002/2013JD021435>
- 497 Pearce, J.L., Beringer, J., Nicholls, N., Hyndman, R.J., Uotila, P., Tapper, N.J., 2011. Investigating the influence of
498 synoptic-scale meteorology on air quality using self-organizing maps and generalized additive modelling.
499 *Atmos. Environ.* 45, 128–136. <https://doi.org/10.1016/j.atmosenv.2010.09.032>
- 500 Ryan, W.F., Doddridge, B.G., Dickerson, R.R., Morales, R.M., Hallock, K.A., Roberts, P.T., Blumenthal, D.L.,
501 Anderson, J.A., Civerolo, K.L., 1998. Pollutant Transport During a Regional O₃ Episode in the Mid-Atlantic
502 States. *J. Air Waste Manage. Assoc.* 48, 786–797. <https://doi.org/10.1080/10473289.1998.10463737>
- 503 Seo, J., Youn, D., Kim, J.Y., Lee, H., 2014. Extensive spatiotemporal analyses of surface ozone and related
504 meteorological variables in South Korea for the period 1999–2010. *Atmos. Chem. Phys.* 14, 6395–6415.
505 <https://doi.org/10.5194/acp-14-6395-2014>
- 506 Sheridan, S.C., 2003. North American weather-type frequency and teleconnection indices. *Int. J. Climatol.* 23, 27–
507 45. <https://doi.org/10.1002/joc.863>
- 508 Sheridan, S.C., 2002. The redevelopment of a weather-type classification scheme for North America. *Int. J.*
509 *Climatol.* 22, 51–68. <https://doi.org/10.1002/joc.709>

510 Sheridan, S.C., Power, H.C., Senkbeil, J.C., 2008. A further analysis of the spatio-temporal variability in aerosols
511 across North America: Incorporation of lower tropospheric (850-hPa) flow. *Int. J. Climatol.* 28, 1189–1199.
512 <https://doi.org/10.1002/joc.1628>

513 Shin, D., Song, S., Ryoo, S.-B., Lee, S.-S., 2020. Variations in Ozone Concentration over the Mid-Latitude Region
514 Revealed by Ozonesonde Observations in Pohang, South Korea. *Atmosphere (Basel)*. 11, 746.
515 <https://doi.org/10.3390/atmos11070746>

516 Sillman, S., 1999. The relation between ozone, NOx and hydrocarbons in urban and polluted rural environments.
517 *Atmos. Environ.* 33, 1821–1845. [https://doi.org/10.1016/S1352-2310\(98\)00345-8](https://doi.org/10.1016/S1352-2310(98)00345-8)

518 Stein, a. F., Draxler, R.R., Rolph, G.D., Stunder, B.J.B.B., Cohen, M.D., Ngan, F., 2015. NOAA’s HYSPLIT Atmospheric
519 Transport and Dispersion Modeling System. *Bull. Am. Meteorol. Soc.* 96, 2059–2077.
520 <https://doi.org/10.1175/BAMS-D-14-00110.1>

521 Stunder, B.J.B., 1996. An Assessment of the Quality of Forecast Trajectories. *J. Appl. Meteorol.* 35, 1319–1331.
522 [https://doi.org/10.1175/1520-0450\(1996\)035<1319:AAOTQO>2.0.CO;2](https://doi.org/10.1175/1520-0450(1996)035<1319:AAOTQO>2.0.CO;2)

523 Sullivan, R.C., Levy, R.C., Pryor, S.C., 2015. Spatiotemporal coherence of mean and extreme aerosol particle events
524 over eastern North America as observed from satellite. *Atmos. Environ.* 112, 126–135.
525 <https://doi.org/10.1016/j.atmosenv.2015.04.026>

526 Sun, L., Xue, L., Wang, Y., Li, L., Lin, J., Ni, R., Yan, Y., Chen, L., Li, J., Zhang, Q., Wang, W., 2019. Impacts of
527 meteorology and emissions on summertime surface ozone increases over central eastern China between
528 2003 and 2015. *Atmos. Chem. Phys.* 19, 1455–1469. <https://doi.org/10.5194/acp-19-1455-2019>

529 Triantafyllou, A., 2001. PM10 pollution episodes as a function of synoptic climatology in a mountainous industrial
530 area. *Environ. Pollut.* 112, 491–500. [https://doi.org/10.1016/S0269-7491\(00\)00131-7](https://doi.org/10.1016/S0269-7491(00)00131-7)

531 Vanos, J.K., Hebborn, C., Cakmak, S., 2014. Risk assessment for cardiovascular and respiratory mortality due to air
532 pollution and synoptic meteorology in 10 Canadian cities. *Environ. Pollut.* 185, 322–332.
533 <https://doi.org/10.1016/j.envpol.2013.11.007>

534 Yun, K.-S., Heo, K.-Y., Chu, J.-E., Ha, K.-J., Lee, E.-J., Choi, Y., Kitoh, A., 2012. Changes in climate classification and
535 extreme climate indices from a high-resolution future projection in Korea. *Asia-Pacific J. Atmos. Sci.* 48, 213–
536 226. <https://doi.org/10.1007/s13143-012-0022-6>

537

538 6. Author contributions

539 Conceptualization; Formal analysis; Methodology; Visualization; H Kim & D Lee, Funding acquisition; S Kim & JH
540 Yoon, Roles/Writing - original draft: HC Kim & D Lee, Writing - review & editing: F. Ngan, B-U Kim, S Kim, C Bae and
541 J-H Yoon

542 7. Acknowledgments

543 This research is funded by the National Research Foundation of Korea under Grant NRF_2017R1A2B4007480, and
544 is also supported by the National Institute of Environment Research (NIER), South Korea (NIER-2019-01-02-034).
545 The Authors greatly appreciate Dr. Sheridan for making the SSC data available (sheridan.geog.kent.edu/ssc.html).

546 8. Disclaimer

547 The scientific results and conclusions, as well as any views or opinions expressed herein, are those of the author(s)
548 and do not necessarily reflect the views of NOAA or the Department of Commerce.

549

550 *Table 1 Frequencies of the SSC weather types in South Korea, 2001–2017. Unit: %*

	DM	DP	DT	MM	MP	MT	MTP	MTDP	Ts
January	30.8	36.7	39.2	37.4	36.6	30.2	9.0	12.3	39.5
February	53.1	39.0	30.9	31.5	20.7	13.7	6.3	3.1	1.0
March	0.0	0.1	1.1	7.1	16.7	27.4	0.2	1.2	5.4
April	15.1	17.6	10.1	4.2	6.5	4.5	3.8	1.8	0.2
May	7.6	10.5	11.1	13.1	16.9	28.9	33.1	20.6	19.3
June	10.2	10.0	6.5	8.6	6.9	4.5	3.1	2.2	1.7
July	1.1	0.7	1.4	1.2	4.0	8.9	0.5	1.2	3.1
August	4.7	8.0	16.8	34.5	35.6	16.7	5.6	3.4	0.4
September	0.2	0.4	0.4	0.3	0.2	0.2	6.2	9.9	1.5
October	0.2	0.3	0.0	0.0	0.1	0.0	0.1	0.1	0.0
November	1.4	2.2	0.1	0.0	0.0	0.0	20.7	22.4	22.6
December	19.9	15.3	11.0	10.4	11.9	15.9	18.8	24.8	25.7
Total	32.8 %	10.7 %	5.9 %	15.7 %	3.7 %	11.0 %	1.7 %	0.3 %	18.2 %

551

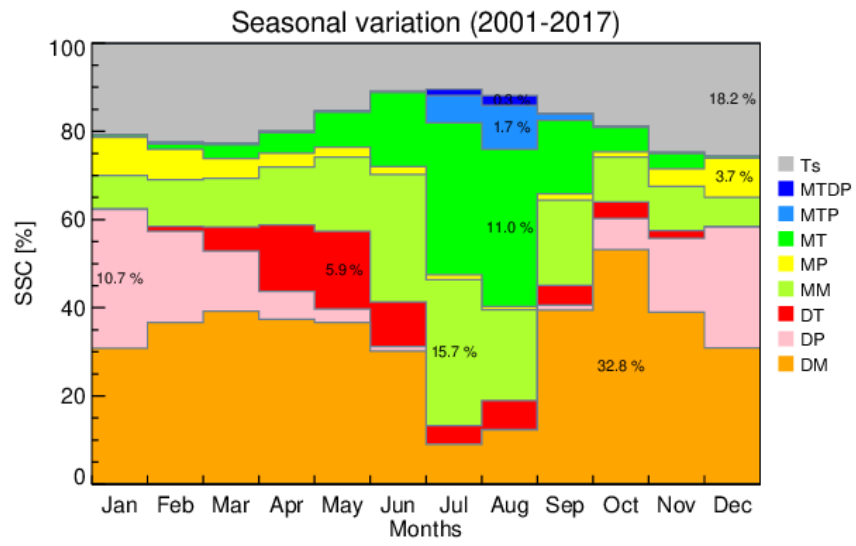
552 *Table 2 Statistics of ozone and meteorological variables for each SSC type.*

	DM	DP	DT	MM	MP	MT	MTP	MTDP	Ts
T (C)	11.11	1.37	17.96	17.19	5.47	22.91	25.91	27.43	10.63
TD (C)	3.91	-7.26	9.41	12.75	0.08	18.46	21.63	23.56	3.83
RH (%)	64.72	56.35	62.43	77.16	70.67	77.88	79.11	81.29	66.49
WS (m/s)	2.14	2.84	2.01	2.10	2.83	1.99	2.11	2.34	2.10
CLD (1-10)	4.22	3.89	3.76	7.43	6.76	6.30	5.76	5.21	5.13
P (hPa)	1017.98	1022.03	1012.44	1012.75	1020.28	1010.08	1009.59	1008.30	1017.12
MDA8									
Ozone (ppb)									
mean	38.8	27.1	57.3	32.3	27.1	41.9	40.4	48.4	36.1
std. dev	18.5	11.1	19.6	14.5	12.8	18.8	19.7	23.3	15.9

553

554

555



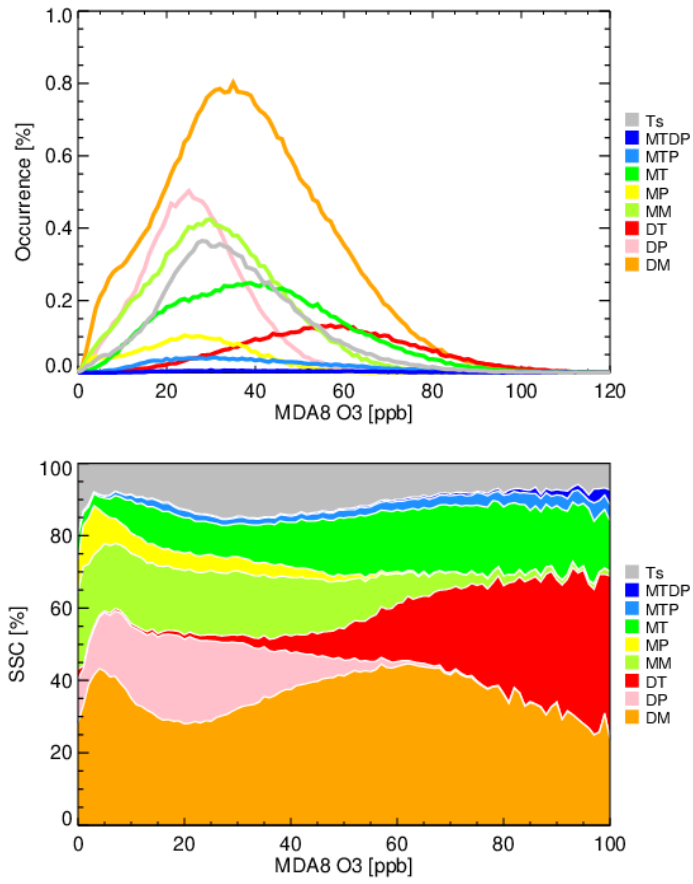
556

557

Figure 1 Seasonal variation of in the SSC types in South Korea, 2001–2017.

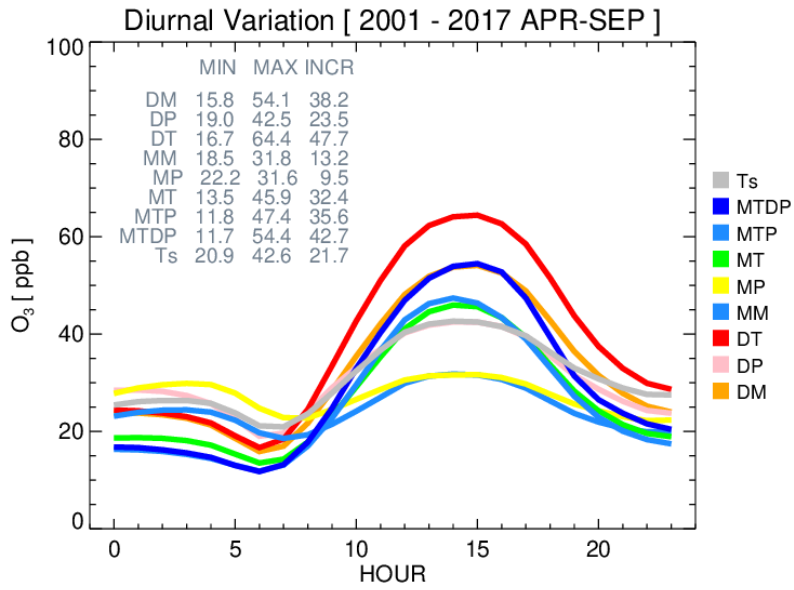
558

559



560
 561
 562
 563
 564

Figure 2 (a) Histogram of the MDA8 ozone frequency distribution for each SSC type in South Korea, 2001–2017. Y-axis is normalized across all data. (b) Fractional coverage of each SSC type in 1 ppb ozone bins.

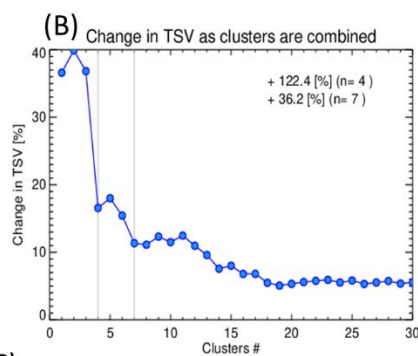
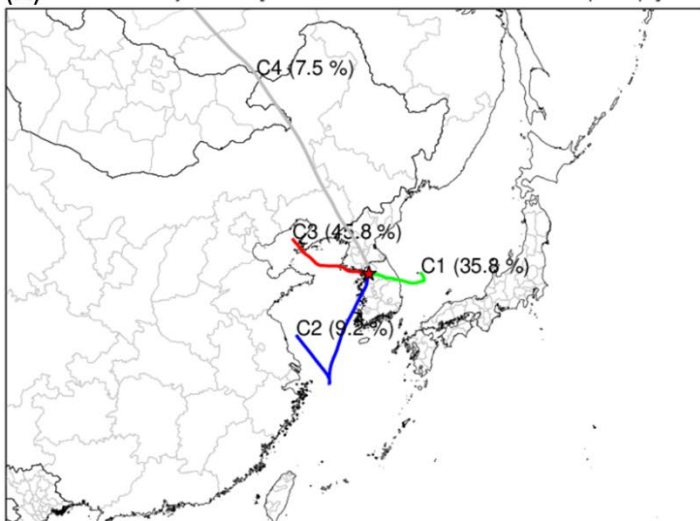


565

566 *Figure 3 Diurnal variations in surface ozone concentrations according to the corresponding SSC types during the*
 567 *2001–2017 warm season (April to September). Minimum, maximum, and increase (i.e., Max-Min) of ozone diurnal*
 568 *variations are also shown for each SSC type (unit: ppb).*

569

(A) Clustered Trajectories [SSC=DT / nclus=4 / 2012-2016 / Apr-Sep]

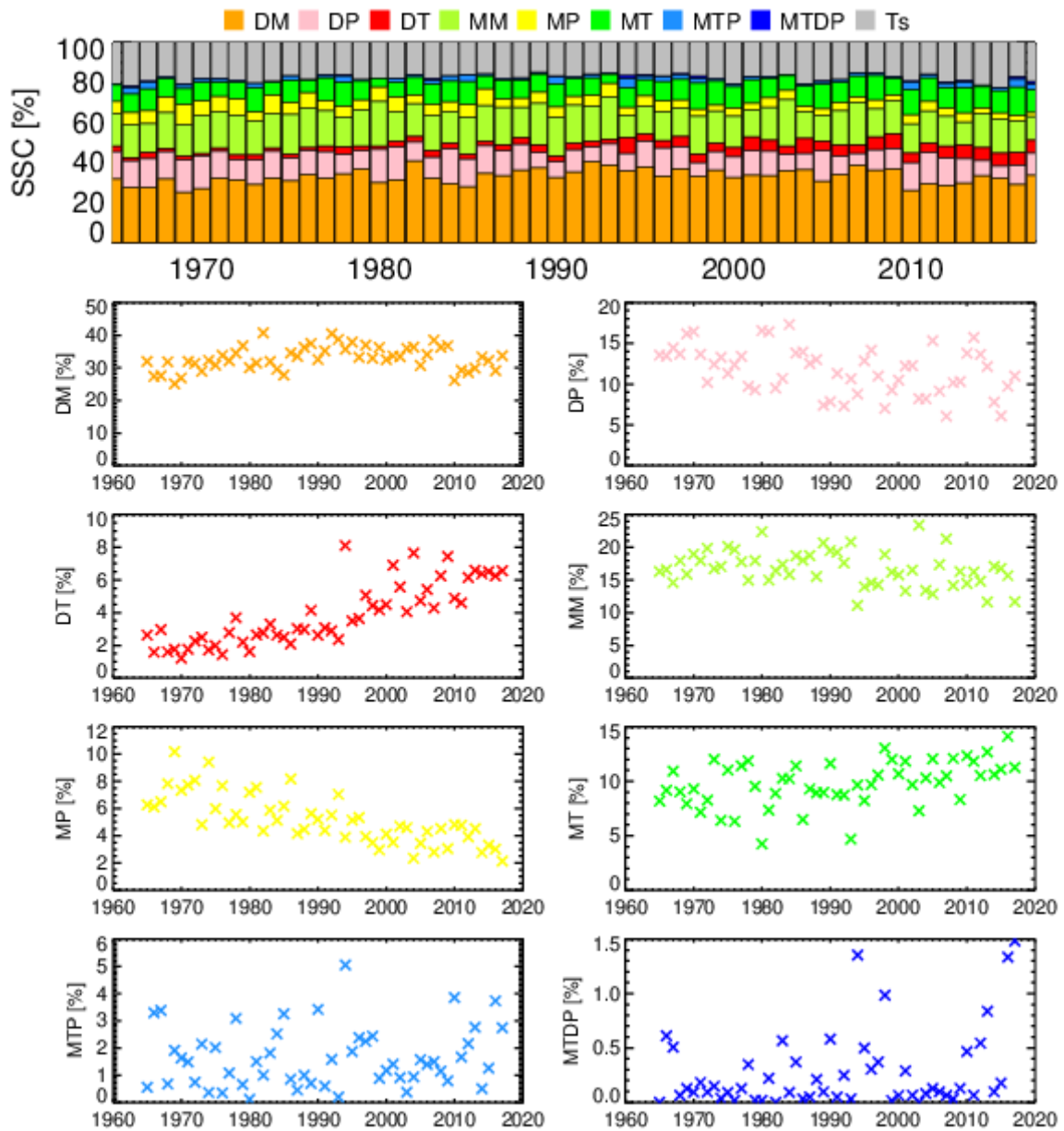


(C)

Cluster	Frequency	MDA8 O3 [SMA]
C1	35.8 %	59.7 ppb
C2	9.2 %	63.2 ppb
C3	45.8 %	59.9 ppb
C4	7.5 %	55.0 ppb

570

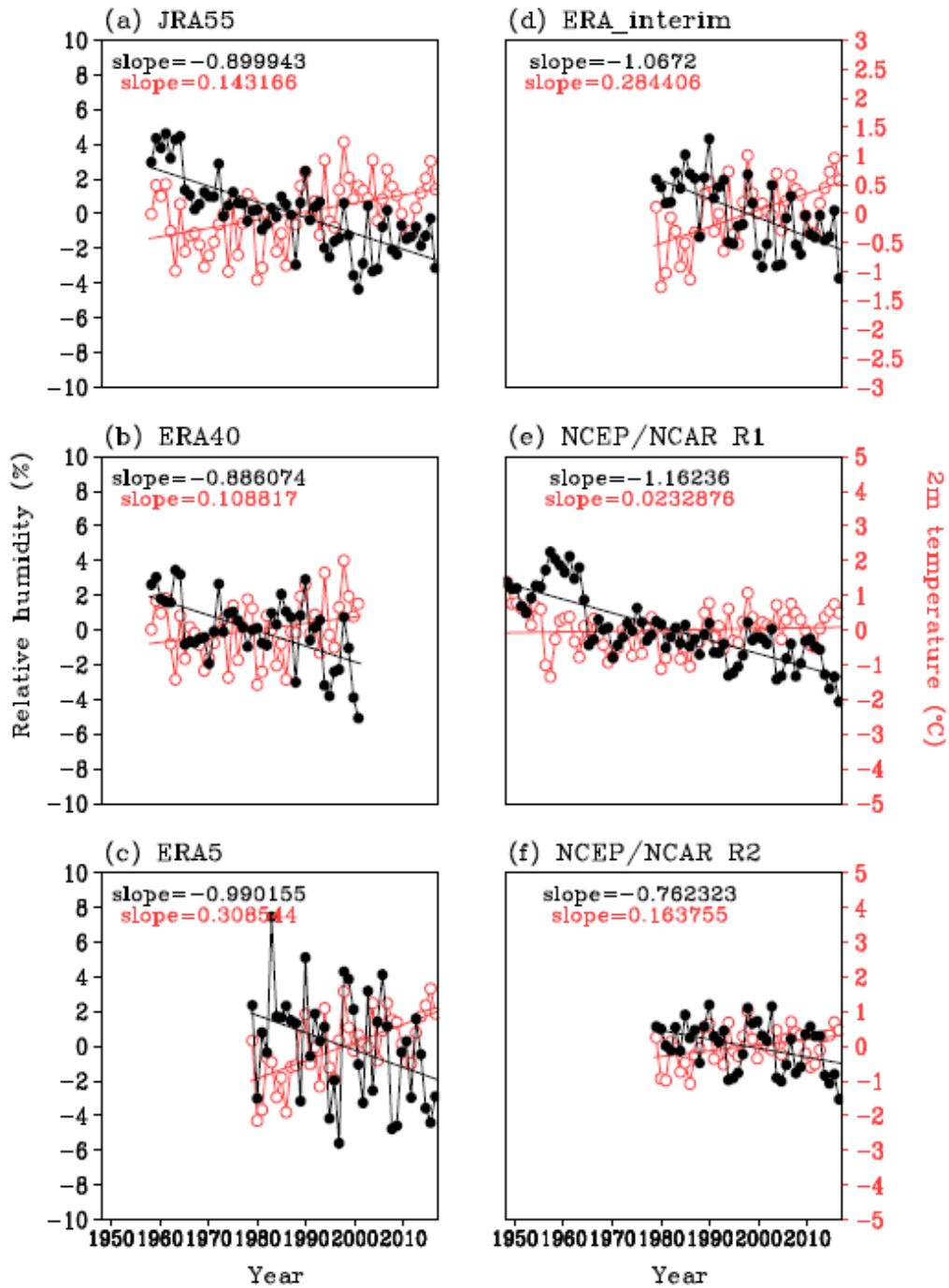
571 *Figure 4 (a) Clustered backward trajectories reaching Seoul, South Korea during the 2012–2016 warm season (April*
572 *to September) for the DT type, (b) Changes in total spatial variances to decide the number of clusters, and (c)*
573 *occurrence frequencies and associated MDA8 ozone concentration for each cluster.*



574

575 *Figure 5 Interannual variation in SSC types in South Korea, 1965–2017. Normalized to total annual counts in each*
 576 *year. Fractional contributions (upper) and individual SSC (lower) are shown.*

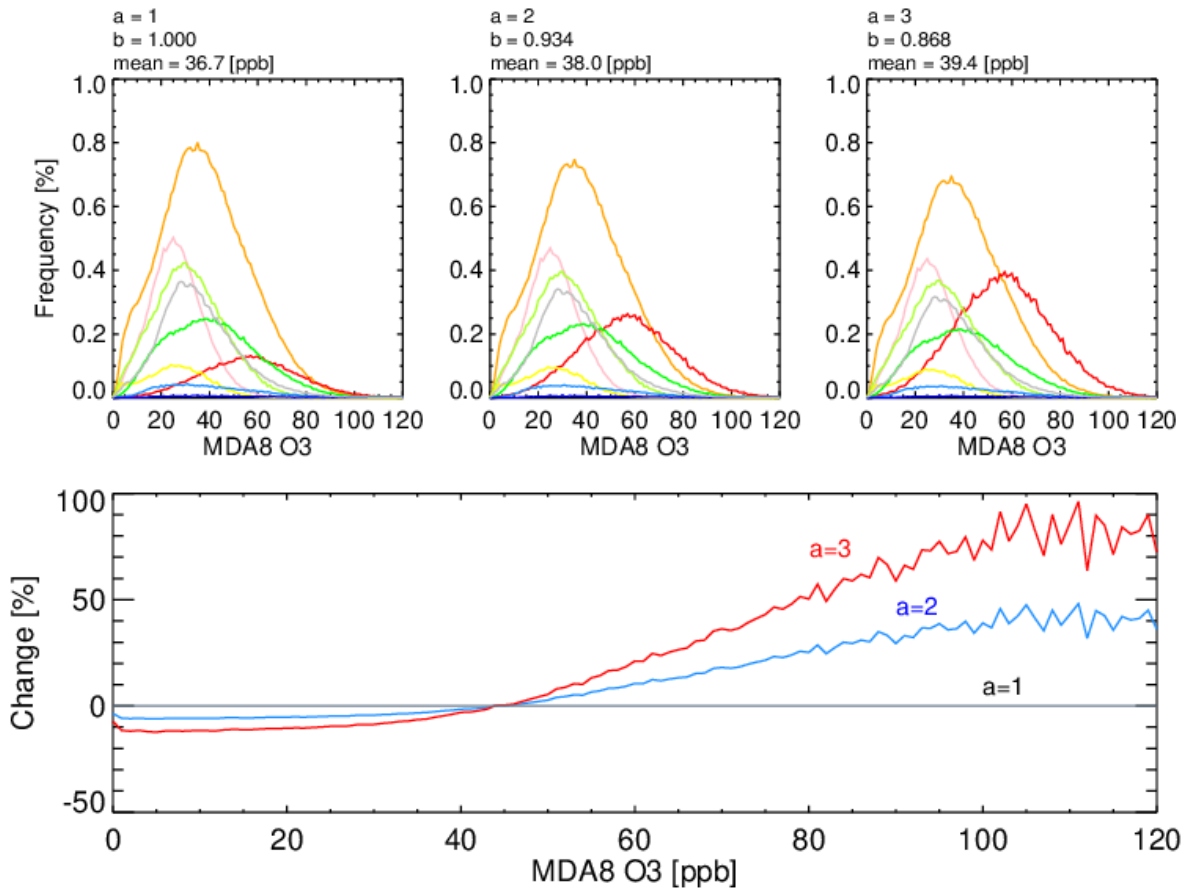
577



578

579 *Figure 6 Interannual variations in 2-m temperature (red line with open circles; °C) and relative humidity (black line*
 580 *with closed circles; %) over South Korea during 1958 – 2017. Anomalies of annual means and their linear fits are*
 581 *calculated using six global reanalysis datasets: (a) JRA-55 (1958 to 2017), (b) MERRA2 (1980 to 2017), (c) ERA5*
 582 *(1979 to 2017), (d) ERA_interim (1979 to 2017), (e) NCEP/NCAR R1 (1958 to 2017), and (f) NCEP/NCAR R2 (1979 to*
 583 *2017). Units for slopes are °C 10 years⁻¹ (2-m temperature) and % 10 years⁻¹ (relative humidity).*

584



585
 586 *Figure 7 Sensitivity tests of adjusting the frequency of the DT type. The changed MDA8 ozone distribution assuming*
 587 *0% (original), 100%, and 200% (i.e., $a=1,2,3$). DT occurrences are shown in the upper panel, and the*
 588 *relative changes in the MDA8 ozone distributions after applying the increased DT are shown in the lower panel.*